Effect of Chronic Hyperglycemia on Glucose Metabolism in Subjects With Normal Glucose Tolerance

Chris Shannon,[1] Aurora Merovci,[1] Juan Xiong,[1] Devjit Tripathy,[1] Felipe Lorenzo,[2] Donald McClain,[2] Muhammad Abdul-Ghani,[1] Luke Norton,[1] and Ralph A. DeFronzo[1]

Chronic hyperglycemia causes insulin resistance, but the inheritability of glucotoxicity and the underlying mechanisms are unclear. We examined the effect of 3 days of hyperglycemia on glucose disposal, enzyme activities, insulin signaling, and protein *O*-GlcNAcylation in skeletal muscle of individuals without (FH⁻) or with (FH⁺) family history of type 2 diabetes. Twenty-five subjects with normal glucose tolerance received a [3-³H]glucose euglycemic insulin clamp, indirect calorimetry, and vastus-lateralis biopsies before and after 3 days of saline (*n* = 5) or glucose (*n* = 10 FH⁻ and 10 FH⁺) infusion to raise plasma glucose by ∼45 mg/dL. At baseline, FH⁺ had lower insulin-stimulated glucose oxidation and total glucose disposal (TGD) but similar nonoxidative glucose disposal and basal endogenous glucose production (bEGP) compared with FH⁻. After 3 days of glucose infusion, bEGP and glucose oxidation were markedly increased, whereas nonoxidative glucose disposal and TGD were lower versus baseline, with no differences between FH⁻ and FH⁺ subjects. Hyperglycemia doubled skeletal muscle glycogen content and impaired activation of glycogen synthase (GS), pyruvate dehydrogenase, and Akt, but protein *O*-GlcNAcylation was unchanged. Insulin resistance develops to a similar extent in FH⁻ and FH⁺ subjects after chronic hyperglycemia, without increased protein *O*-GlcNAcylation. Decreased nonoxidative glucose disposal due to impaired GS activation appears to be the primary deficit in skeletal muscle glucotoxicity.

Insulin resistance is a core defect in type 2 diabetes (T2D) (1,2) and is the first metabolic abnormality detected in subjects destined to develop T2D (3,4). Insulin-resistant individuals manifest diminished insulin-stimulated glucose disposal in skeletal and cardiac muscle (5–7), adipocytes (8), liver (9), and gastrointestinal tract (10). In skeletal muscle, the defect in insulin action involves multiple intracellular steps in glucose metabolism, including glucose oxidation and glycogen synthesis (1,2,11,12). The etiology of insulin resistance is complex and includes both genetic and acquired factors (2).

Studies in experimental animals (13,14) and in man (15,16) have demonstrated that chronic elevation in the plasma glucose concentration impairs insulin action, i.e., glucotoxicity (17). Lowering the plasma glucose concentration with insulin therapy (18) or by inhibition of renal glucose absorption (19) improves insulin sensitivity in individuals with T2D. The improvement in insulin sensitivity observed with intensive insulin therapy was due to an increase in nonoxidative glucose disposal (18), suggesting that glucotoxicity impairs insulin action by impairing glycogen synthesis. However, the molecular events underlying the development of insulin resistance and alterations in intracellular glucose metabolism in response to glucotoxicity remain poorly characterized.

Glycogen synthase (GS) and pyruvate dehydrogenase (PDH) are the rate-limiting enzymes in the regulation of nonoxidative glycogen synthesis and glucose oxidation, respectively. An additional route of skeletal muscle glucose metabolism involves synthesis of the hexosamine product *O*-linked β-*N*-acetylglucosamine (*O*-GlcNAc), a pathway that appears to be upregulated in T2D and has previously been implicated in the development of insulin resistance and glucotoxicity (20–22). Prior studies suggest that both GS (23) and PDH (24) may be modulated by *O*-GlcNAcylation

METABOLISM

[1]Division of Diabetes, University of Texas Health Science Center and Texas Diabetes Institute, San Antonio, TX

[2]Center on Diabetes, Obesity, and Metabolism, Wake Forest University, Winston-Salem, NC

Corresponding author: Ralph A. DeFronzo, albarado@uthscsa.edu.

and thus could be sensitive to increased *O*-GlcNAc synthesis, but whether *O*-GlcNAc levels respond to chronic hyperglycemia in humans is unclear. Therefore, the aim of the current study was to examine the effect of chronic (3 days) elevation of the plasma glucose concentration on oxidative and nonoxidative glucose disposal, as well as the prospective involvement of GS, PDH, and *O*-GlcNAcylation, in lean healthy subjects with normal glucose tolerance (NGT) with and without family history (FH) of diabetes. We hypothesized that experimental hyperglycemia would alter the intracellular pathways of glucose metabolism in NGT subjects and, based upon previous studies (25), that these changes would be more pronounced in subjects with FH of diabetes.

RESEARCH DESIGN AND METHODS

Subjects

Twenty-five NGT subjects (15 without FH of T2D and 10 with FH) participated in the study. All subjects were in good general health as determined by medical history, physical exam, screening lab tests, urinalysis, and EKG. Body weight was stable ($\pm$3 lb) in all subjects for 3 months prior to the study and no subject was considered excessively active or sedentary. No subject was taking any medication known to affect glucose metabolism. FH^+ was defined as two or more first-degree relatives (mother, father, siblings, or children) with T2D, ascertained by recall during the screening visit. FH^- subjects (including saline control subjects) had no first-degree relatives with T2D.

Research Design

All studies were performed at the Clinical Research Center (CRC) at the South Texas Veterans Health Care System at 7:00 A.M. after a 10-h overnight fast and after abstention from strenuous exercise or alcohol consumption for 48 h. After screening, eligible subjects received a 4-h euglycemic insulin clamp (26) with indirect calorimetry, vastus lateralis muscle biopsies, and [3-^{3}H]glucose infusion. Skeletal muscle biopsies were obtained from the vastus lateralis muscle $\sim$1 h prior to and at the end of the insulin clamp and were snap frozen in liquid nitrogen. Within 7 days, subjects returned to the CRC for a 3-day continuous glucose (n = 20) or saline (n = 5) infusion study. At 7:00 A.M. on day 4, the glucose infusion was discontinued and the euglycemic insulin clamp with indirect calorimetry, [3-^{3}H]glucose, and vastus lateralis muscle biopsy was repeated.

Euglycemic Insulin Clamp

A catheter was placed into an antecubital vein for the infusion of all test substances. A second catheter was inserted retrogradely into a vein on the dorsum of the hand, and the hand was placed into a thermoregulated box heated to 70°C. All subjects received a prime (40 μCi)-continuous (0.4 μCi/min) infusion of [3-^{3}H]glucose (DuPont NEN; Life Science Products, Boston, MA). After a 2-h basal tracer equilibration period, subjects received a prime-continuous insulin infusion at the rate of

80 mU/m^2 · min. During the last 30 min of the basal equilibration period and throughout the insulin infusion, plasma samples were taken at 5–10-min intervals for determination of plasma glucose and insulin concentrations and tritiated glucose radioactivity. During the insulin infusion, a variable infusion of 20% glucose was adjusted, based on the negative feedback principle, to maintain the plasma glucose concentration at $\sim$100 mg/dL with a coefficient of variation <5%.

Three-Day Glucose Infusion

Subjects were admitted at 8:00 A.M. for the 3-day glucose (n = 20) or saline (n = 5) infusion study. A catheter was placed into an antecubital vein and a variable infusion of 20% glucose was started to raise and maintain the plasma glucose concentration to $\sim$45 mg/dL above the fasting level. Plasma glucose was measured every 5–30 min, and the glucose infusion rate was adjusted to maintain the plasma glucose concentration at the target $\pm$5 mg/dL. Fasting plasma insulin, free fatty acid (FFA), and C-peptide were measured in the morning of days 1, 2, 3, and 4. On the morning of day 4, the glucose infusion was discontinued, at which time the prime-continuous infusion of [3-^{3}H]glucose was initiated. The plasma glucose concentration was subsequently allowed to return to the fasting level, at which time the euglycemic insulin clamp with vastus lateralis muscle biopsy, tritiated glucose, and indirect calorimetry was then repeated. In all subjects, the plasma glucose concentration returned to the baseline fasting level within 2–3 h and the glucose specific activity was constant for 30 min prior to insulin infusion (see Supplementary Fig. 1). During the glucose infusion period, subjects received a standardized diet (55% carbohydrate, 30% fat, and 15% protein) with calories divided as 20% for breakfast and 40% each for lunch and dinner. Breakfast was not permitted on the morning of day 4. Subjects were encouraged to ambulate during the 3-day glucose infusion period.

Analytical Determinations

Plasma glucose concentration was determined by the glucose oxidase method (Analox Glucose Analyzer; Analox Instruments, Lunenburg, MA). Plasma insulin concentration was determined by radioimmunoassay (Diagnostic Products, Los Angeles, CA). Plasma tritiated glucose radioactivity was determined on barium hydroxide/zinc sulfate–precipitated plasma extracts. An $\sim$20-mg portion of muscle was analyzed for PDH activation status (27). An aliquot of homogenate was removed and frozen for the determination of the expression level of the following proteins by Western blotting: PDH E1α (3205; Cell Signaling Technology [CST]), pE1α (Ser^{293}, 92696; Abcam), PDH kinase 4 (PDK4) (110336; Abcam), Akt (4691; CST), pAkt (Ser^{473}, 9271; CST), GS (3886; CST), pGS (Ser^{641}, 3891; CST), GS kinase 3β (GSK3β) (9315; CST), pGSK3β (Ser^9, 9323; CST), glutamine:fructose-6-phoshate amidotransferase 1 (GFAT1) (5322; CST), and *O*-GlcNAc transferase (OGT) (24083; CST). Global protein *O*-GlcNAcylation was assessed by Western blotting using the CTD110.6

Table 1—Baseline patient characteristics

	FH$^-$	FH$^+$	Control
Number	10	10	5
Age (years)	45 ± 4	43 ± 5	49 ± 4
Sex (male/female)	7/3	6/4	2/3
Ethnicity (Mexican American/ Caucasian/ African American)	3/4/3	6/3/1	1/4
BMI (kg/m^2)	24.3 ± 1.1	26.1 ± 1.2	24.5 ± 1.3
Body weight (kg)	75.6 ± 16.3	73.7 ± 10.9	72.6 ± 11.5
Fat-free mass (kg)	57.4 ± 12.8	51.5 ± 9.6	52.0 ± 11.2
HbA$_{1c}$ (%)	5.4 ± 0.1	5.4 ± 0.1	5.4 ± 0.1
FPG (mg/dL)	96.2 ± 2.6	100.7 ± 2.0	94.1 ± 5.2
2-h plasma glucose (mg/dL) OGTT	95 ± 5	109 ± 6	111 ± 5

Data are mean ± SD or n. There were no significant differences between the FH$^-$, FH$^+$, and control groups.

antibody (9875; CST), with visible bands quantified individually and summed for each lane. A second portion of muscle (~50 mg) was freeze-dried and extracted in 0.5 mol/L perchloric acid followed by alkaline digestion for the determination of acid-soluble and acid-insoluble metabolites (28). Glucose-6-phosphate (G6P) was assayed by the fluorometric detection of NADH in the presence of 50 mmol/L triethanolamine, 0.5 mmol/L dithiothreitol, 0.25 mmol/L ATP, 1 mmol/L NAD, and 0.6 units bacterial G6PDH (G5760; Sigma-Aldrich). Glycogen (28) and long-chain acyl CoA (LCAC) (29) were measured as described previously.

Calculations and Statistical Analysis

The basal rate of endogenous (primarily hepatic) glucose production (bEGP) was calculated as the [3-^{3}H]glucose infusion rate (dpm/min) divided by the steady-state plasma [3-^{3}H]glucose specific activity (dpm/mg). After insulin infusion, nonsteady-state conditions for [3-^{3}H]-glucose prevail and total rate of glucose appearance (R_a) in the systemic circulation was computed using Steele's equation during the last 30 min of the 4-h insulin clamp, assuming a constant distribution volume of 250 mg/kg body weight (30). The residual rate of EGP (rEGP) during the last 30 min of the clamp step was calculated by subtracting the glucose infusion rate from R_a during the same time period. Indirect calorimetry was performed during the 30 min before the start of the clamp (−30 to 0 min) and during the last 30 min of the insulin infusion (210–240 min). Glucose and lipid oxidation were calculated using the nonprotein respiratory exchange ratio (RER) (31). Nonoxidative glucose disposal was calculated by subtracting the rate of glucose oxidation from total glucose disposal (TGD) during the insulin clamp. Units for glucose production, glucose oxidation, and nonoxidative glucose disposal are normalized to body weight, given as
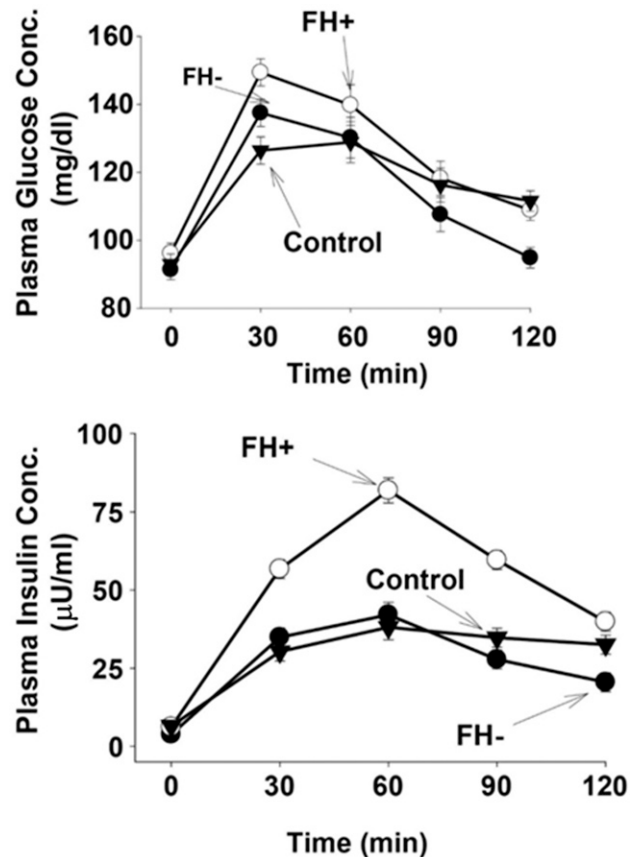

Figure 1—Plasma glucose and insulin concentrations during the OGTT performed in NGT individuals with (FH$^+$) and without (FH$^-$) FH of diabetes and in the NGT control group.

milligrams of glucose per kilogram body weight per minute (mg/kg · min). Values are presented as the mean ± SE. Differences between means were tested with repeated and mixed-model ANOVA, as described in the figure legends. Statistical significance was determined at $P < 0.05$.

RESULTS

Subject Characteristics and Oral Glucose Tolerance Test

Table 1 presents baseline patient characteristics. Subjects were well matched for age, BMI, and sex. FH$^+$ subjects had a slightly, although not significantly, higher fasting plasma glucose (FPG) concentration and rise in plasma glucose concentration during the oral glucose tolerance test (OGTT) (Fig. 1). Consistent with previous studies, FH$^+$ subjects had significantly greater increase in plasma insulin concentration during the OGTT (Fig. 1). Body weight and BMI were similar in FH$^-$, FH$^+$, and control groups.

Baseline Euglycemic Insulin Clamp

During the baseline insulin clamp, the steady-state plasma insulin (163 ± 2 vs. 172 ± 12 μU/mL) and glucose (94.8 ± 1.8 vs. 95.9 ± 1.6) concentrations were similar in FH$^-$ and FH$^+$ groups, respectively. During the baseline insulin

clamp, bEGP was comparable in FH⁻ and FH⁺ subjects, and rEGP during the insulin clamp was similarly suppressed in both groups (Table 2).

Consistent with previous studies (3), FH⁺ subjects had a significantly lower rate of total body insulin-stimulated glucose disposal during the baseline insulin clamp compared with FH⁻ subjects (Table 2). The basal rate of glucose oxidation was comparable in FH⁺ and FH⁻ groups, but during the insulin clamp, glucose oxidation increased more ($P < 0.05$) in FH⁻ subjects (by 105%) than in FH⁺ subjects (by 64%) (Table 2).

After 3-Day Glucose Infusion
FPG concentration on day 1 before the start of glucose infusion was 95 ± 3 and 102 ± 2 mg/dL in FH⁻ and FH⁺ subjects, respectively ($P = 0.05$), and increased similarly on days 2, 3, and 4 in FH⁺ and FH⁻ subjects (144 ± 6 vs. 148 ± 7, 139 ± 4 vs. 148 ± 3, and 139 ± 4 vs. 135 ± 98 mg/dL, respectively; all $P < 0.001$ vs. baseline) (Fig. 2). After stopping the glucose infusion on day 4, the plasma glucose concentration decreased to 100 ± 2 and 99 ± 3 mg/dL in FH⁻ and FH⁺ subjects, respectively, prior to the start of the repeat insulin clamp study. Fasting plasma insulin concentration before the start of glucose infusion was 8 ± 3 and 12 ± 2 μU/mL in FH⁻ and FH⁺, respectively ($P > 0.3$), and progressively increased to 26 ± 6 vs. 44 ± 7, 49 ± 15 vs. 61 ± 9, and 52 ± 15 vs. 65 ± 11 on days 2, 3,

and 4 in FH⁻ and FH⁺ subjects, respectively (all $P < 0.05$ vs. baseline and $P = $ NS for FH⁻ vs. FH⁺) (Fig. 2). Fasting plasma FFA before the start of glucose infusion was 0.50 ± 0.06 and 0.45 ± 0.06 mmol/L in FH⁻ and FH⁺, respectively, and was suppressed similarly to 0.08 ± 0.01 vs. 0.06 ± 0.01, 0.06 ± 0.01 vs. 0.07 ± 0.01, and 0.07 ± 0.01 vs. 0.07 ± 0.02 mmol/L on days 2, 3, and 4 (Fig. 2).

In subjects who received saline infusion, the FPG, fasting plasma insulin, and fasting plasma FFA concentrations remained unchanged throughout the study period (Fig. 2).

Effect of Glucose Infusion on Insulin Sensitivity
The FPG concentration in the morning of day 4 (before the start of the repeat insulin clamp) was comparable in FH⁻ and FH⁺ groups: 100 ± 2 and 99 ± 3 mg/dL, respectively. bEGP increased markedly after 3 days of glucose infusion ($P < 0.001$, vs. baseline) and was comparable in FH⁻ and FH⁺ groups (Table 2). The basal rate of glucose oxidation was significantly increased in both groups after glucose infusion, whereas the basal rate of lipid oxidation was decreased markedly ($P < 0.001$) in both groups (Table 2).

During the insulin clamp performed after 3 days of glucose infusion, the steady-state plasma glucose (96 ± 2, 98 ± 1, and 97 ± 2 mg/dL) concentrations were similar to those in the baseline study in FH⁻, FH⁺, and control groups, respectively, whereas the steady-state plasma insulin concentration increased similarly and significantly

Table 2—TGD, nonoxidative glucose disposal, glucose oxidation, and rEGP (primarily reflects hepatic) during the insulin clamp before and after glucose infusion

	FH⁻	FH⁺	Control
Baseline insulin clamp			
Steady-state plasma glucose (mg/dL)	94.8 ± 1.8	95.9 ± 1.6	94.9 ± 3.3
Steady-state plasma insulin (μU/mL)	163 ± 2	172 ± 12	125 ± 8
bEGP (mg/kg/min)	2.33 ± 0.08	2.09 ± 0.09	2.46 ± 0.11
bEGP × basal insulin ([μU/mL] · [mg/kg/min])	20.5 ± 1.9	19.3 ± 4.2	19.2 ± 1.7
TGD (mg/kg/min)	11.49 ± 0.91	9.32 ± 0.49*	11.18 ± 1.64
rEGP (mg/kg/min)	0.56 ± 0.2	0.56 ± 0.33	0.34 ± 0.26
Basal glucose oxidation (mg/kg/min)	1.33 ± 0.13	1.14 ± 0.18	1.34 ± 0.13
Clamp glucose oxidation (mg/kg/min)	2.75 ± 0.53	1.81 ± 0.26*	2.45 ± 0.17
Nonoxidative glucose disposal (mg/kg/min)	8.69 ± 0.82	7.46 ± 0.61	8.35 ± 1.88
Basal LOX (mg/kg/min)	0.92 ± 0.10	0.94 ± 0.09	0.99 ± 0.19
Clamp LOX (mg/kg/min)	0.50 ± 0.08	0.74 ± 0.11	0.45 ± 0.2
Basal RER	0.81 ± 0.02	0.80 ± 0.02	0.81 ± 0.02
Clamp RER	0.90 ± 0.02	0.85 ± 0.02	0.91 ± 0.03
Insulin clamp post–glucose infusion			
Steady-state plasma glucose (mg/dL)	96.1 ± 2.0	98.1 ± 1.4	96.9 ± 2.0
Steady-state plasma insulin (μU/mL)	208 ± 24	198 ± 10	121 ± 8
bEGP (mg/kg/min)	3.87 ± 0.37††	3.63 ± 0.27††	2.27 ± 0.11
bEGP × basal insulin ([μU/mL] · [mg/kg/min])	74.9 ± 12.8††	59.1 ± 5.5†††	20.4 ± 1.0
TGD (mg/kg/min)	9.46 ± 0.69†††	8.12 ± 0.55††	10.65 ± 1.61
rEGP (mg/kg/min)	0.54 ± 0.22	0.47 ± 0.11	0.14 ± 0.09
Basal glucose oxidation (mg/kg/min)	4.64 ± 0.39	3.78 ± 0.25	1.35 ± 0.18
Clamp glucose oxidation (mg/kg/min)	5.12 ± 0.37†	4.39 ± 0.29†	3.03 ± 0.21
Nonoxidative glucose disposal (mg/kg/min)	4.28 ± 0.60†	4.11 ± 0.69†	7.61 ± 1.69
Basal LOX (mg/kg/min)	−0.14 ± 0.12	0.14 ± 0.06	0.86 ± 0.04
Clamp LOX (mg/kg/min)	−0.15 ± 0.12	0.09 ± 0.08	0.42 ± 0.11
Basal RER	1.0 ± 0.02	0.97 ± 0.01	0.81 ± 0.01
Clamp RER	1.0 ± 0.02	0.98 ± 0.01	0.92 ± 0.01

Data are mean ± SE. LOX, lipid oxidation. *$P < 0.05$, FH⁺ vs. FH⁻. †$P < 0.001$, post–glucose infusion vs. baseline. ††$P = 0.08$, post–glucose infusion vs. baseline. †††$P = 0.02$, post–glucose infusion vs. baseline.
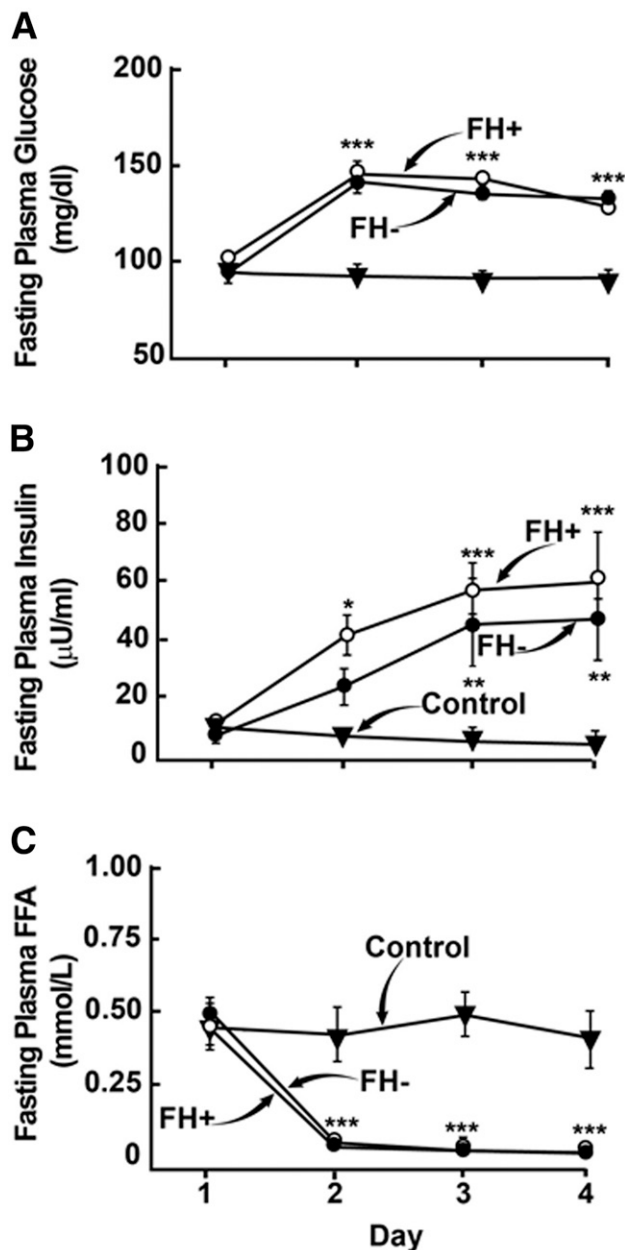
Figure 2—FPG (*A*), insulin (*B*), and FFA (*C*) concentrations at baseline and during 3 days of either glucose infusion in NGT individuals without (FH$^-$, *n* = 10) and with (FH$^+$, *n* = 10) FH of diabetes, or saline infusion in the NGT control group (*n* = 5). Data represent mean ± SE and were analyzed using two-way mixed-model (group × time) ANOVA. *$P < 0.05$, **$P < 0.01$, and ***$P < 0.001$, vs. control group and vs. baseline.

in FH$^-$ (208 ± 24) and FH$^+$ (198 ± 10) versus control (121 ± 8 µU/mL) groups.

After 3 days of glucose infusion, total-body insulin-mediated glucose disposal was significantly decreased in FH$^-$ subjects (from 11.49 ± 0.9 to 9.46 ± 0.69 mg/kg · min, $P = 0.02$), whereas a modest, nonsignificant decrease was observed in FH$^+$ subjects (from 9.32 ± 0.0.49 to 8.12 ± 0.55, $P = 0.08$) (Table 2 and Fig. 3). Despite the decrease in TGD in FH$^-$ subjects, glucose oxidation during

insulin infusion was markedly increased (from 2.75 ± 0.53 to 5.12 ± 0.37 mg/kg · min, $P < 0.0001$), whereas nonoxidative glucose disposal was markedly diminished (8.69 ± 0.72 to 4.28 ± 0.60 mg/kg · min, $P < 0.001$). Although TGD was not significantly reduced by glucose infusion in FH$^+$ subjects, oxidative (increased) and non-oxidative (decreased) glucose disposal were affected similarly to those in FH$^-$ subjects; oxidative glucose disposal increased by 142% ($P < 0.001$) and nonoxidative glucose disposal decreased by 45% ($P < 0.001$) in FH$^+$ subjects (Table 2 and Fig. 3).

In control subjects, bEGP, suppression of EGP during the insulin clamp, and insulin-stimulated TGD, glucose oxidation, and nonoxidative glucose disposal did not differ after 3 days of saline infusion (Table 2).

Skeletal Muscle Responses to Glucose Infusion
Consistent with the finding that both oxidative and non-oxidative pathways of glucose metabolism were similarly altered in FH$^-$ and FH$^+$ subjects after glucose infusion, skeletal muscle biopsy molecular analyses revealed no differences between FH$^-$ and FH$^+$ groups after experimental hyperglycemia (Supplementary Fig. 2). As such, the main effects of glucose infusion are presented collectively for FH$^-$ and FH$^+$ subjects for clarity.

GS Regulation
Nonoxidative glucose disposal in skeletal muscle primarily represents glycogen synthesis (32). During the insulin clamp performed prior to the 3-day glucose infusion, muscle glycogen (mmol/kg dry weight) increased from 341 ± 34 to 430 ± 43 and 347 ± 19 to 400 ± 33 in FH$^-$ and FH$^+$ subjects, respectively (both $P < 0.05$) (Fig. 4A).

After 3 days of glucose infusion, muscle glycogen was increased by ~100% in both FH$^-$ and FH$^+$ groups ($P < 0.0001$) but remained stable in the saline infusion control subjects (Fig. 4A). GS phosphorylation (Ser^{641}) after glucose infusion was also increased, both under basal conditions and during the insulin clamp ($P = 0.03$) (Fig. 4B). Moreover, phosphorylation of GSK3β (Ser^9), the primary isoform of the regulatory GSK in skeletal muscle, tended to be reduced ($P = 0.07$) (Fig. 4C). Together, these observations are consistent with an overall inhibition of GS activation. Skeletal muscle levels of G6P were unchanged after glucose infusion (Fig. 4D).

PDH Activation
The PDH complex represents a key regulatory enzymatic step in the intracellular fate of glucose, coupling glycolytic and oxidative pathways of carbohydrate metabolism. Consistent with the increased rate of glucose oxidation, the protein expression of PDK4, the primary kinase responsible for the phosphorylation and inactivation of skeletal muscle PDH, was reduced by 61% ($P < 0.001$) after glucose infusion (Fig. 5A). Despite the reduction in PDK4, phosphorylation (Ser^{293}) of the E1α subunit of PDH was unchanged (Fig. 5B), and in agreement with the latter, the basal activation status of PDH was comparable to baseline (i.e., before glucose
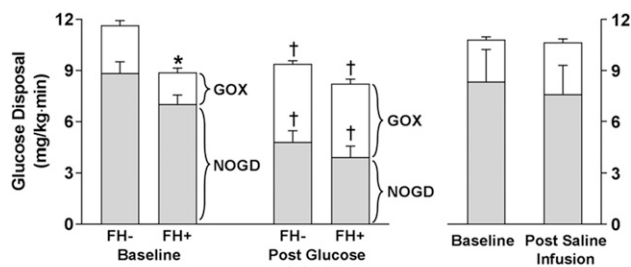
Figure 3—Insulin-stimulated TGD (total height of bars), nonoxidative glucose disposal (NOGD) (shaded part of bars), and glucose oxidation (GOX) in FH$^+$ and FH$^-$ individuals during the euglycemic insulin clamp performed at baseline and after 3 days of glucose infusion. Right panel shows control subjects receiving saline infusion. *$P <$ 0.05, FH$^+$ vs. FH$^-$; †$P <$ 0.05, postglucose infusion vs. baseline.

infusion) (Fig. 4C). However, glucose infusion resulted in a 20% reduction in insulin-stimulated PDH activation compared with baseline (P = 0.02) (Fig. 4C).

Insulin Signaling

To examine whether the perturbed activation of GS and PDH after glucose infusion could be related to upstream insulin signaling events, we measured muscle Akt protein phosphorylation. During the baseline insulin clamp performed prior to glucose infusion, insulin increased muscle Akt phosphorylation (Ser473) by 12-fold ($P <$ 0.001) (Fig. 5D). However, insulin-stimulated Akt phosphorylation was blunted by 27% (P = 0.03) after glucose infusion, compared with baseline (Fig. 5D).

Given the association between the accumulation of toxic lipid intermediates and the development of skeletal muscle insulin resistance (6), particularly under conditions of increased carbohydrate availability, we also measured the total content of LCAC. However, glucose infusion had no impact upon either the basal (7.8 ± 1.3 vs. 7.0 ± 1.0, P = 0.2) or insulin-stimulated (10.4 ± 1.7 vs. 7.1 ± 0.8 μmol/kg dry weight, P = 0.2) concentrations of LCAC.

GFAT, OGT, and Protein O-GlcNAcylation

Prior evidence has suggested a role for the hexosamine biosynthesis pathway in the development of skeletal muscle insulin resistance, particularly through the posttranslational modification of proteins by O-GlcNAcylation (33). However, we found that 3 days of glucose infusion had no impact on global O-GlcNAcylated protein levels in skeletal muscle (Fig. 6A and B). We also measured the protein levels of GFAT1, the first and rate-limiting enzyme in hexosamine biosynthesis, as well as OGT, the rate-limiting enzyme in protein O-GlcNAcylation. Consistent with the lack of increase in O-GlcNAc levels, neither GFAT1 (Fig. 6C) nor OGT (Fig. 6D) protein expression were altered after 3 days of glucose infusion.

DISCUSSION

The results of the current study demonstrate that a small physiologic (~45 mg/dL) elevation in plasma glucose concentration for only 3 days exerts multiple and marked effects on hepatic and peripheral glucose metabolism in lean healthy NGT individuals with and without FH of T2D. Although the reduction in insulin-stimulated TGD did not reach statistical significance in the FH$^-$ group (13% decrease, P = 0.08), the directional change was similar to that in the FH$^+$ group (18% decrease, $P <$ 0.001), and both insulin-stimulated glucose oxidation and nonoxidative glucose disposal were similarly and significantly affected by hyperglycemia in both groups. Thus, hyperglycemia caused a marked increase in insulin-stimulated glucose oxidation in both groups (86% and 142% in FH$^-$ and FH$^+$ subjects, respectively) and a marked decrease in nonoxidative glucose disposal, which primarily represents glycogen synthesis (by 50% and 45% in FH$^-$ and FH$^+$ subjects, respectively). These results demonstrate that hyperglycemia exerts similar deleterious effects on the intracellular pathways of glucose disposal in subjects with and without FH of diabetes. The small quantitative difference in insulin-stimulated TGD between the two groups after 3 days of experimental hyperglycemia most likely is explained by the greater degree of insulin resistance in the FH$^+$ group observed during the baseline insulin clamp, reflecting differences in inheritable (and/or environmental) factors between the two groups. Importantly, no changes in insulin-stimulated TGD, glucose oxidation, or nonoxidative glucose disposal were observed in the control group, who were treated in an identical fashion as the glucose-infused groups with the exception that they received an infusion of normal saline. This distinguishes the effects of experimental hyperglycemia from the possible influence of decreased activity during the 3-day glucose infusion period.

The results of the current study are consistent with a previous study from our group that demonstrated that a small increase (+20 mg/dL) in plasma glucose concentration in NGT FH$^-$ subjects caused a significant increase (~25%) in glucose oxidation and decrease (~35%) in nonoxidative glucose disposal (16). The greater magnitude of change in both oxidative and nonoxidative glucose disposal in FH$^-$ subjects in the current study most likely is explained by the longer duration of hyperglycemia (3 days in the current study vs. 2 days in the previous study) and greater increment in plasma glucose concentration (45 vs. 20 mg/dL). Thus, the results of the current study are consistent with our previous study and extend them to demonstrate that 1) there is a dose-response relationship between the level of hyperglycemia and its impact on both oxidative and nonoxidative glucose disposal, and 2) hyperglycemia affects oxidative and nonoxidative glucose disposal similarly in FH$^+$ and FH$^-$ subjects.

Chronic elevation of plasma glucose concentration had a dramatic effect on bEGP, which was elevated by 66% and 73% in FH$^-$ and FH$^+$ groups, respectively, despite a marked increase in the fasting plasma insulin concentration (59 vs. 10 μU/mL, $P <$ 0.001). The results indicate that hepatic insulin resistance was induced by sustained elevation of the plasma glucose concentration. This represents a novel finding and demonstrates that chronic experimental
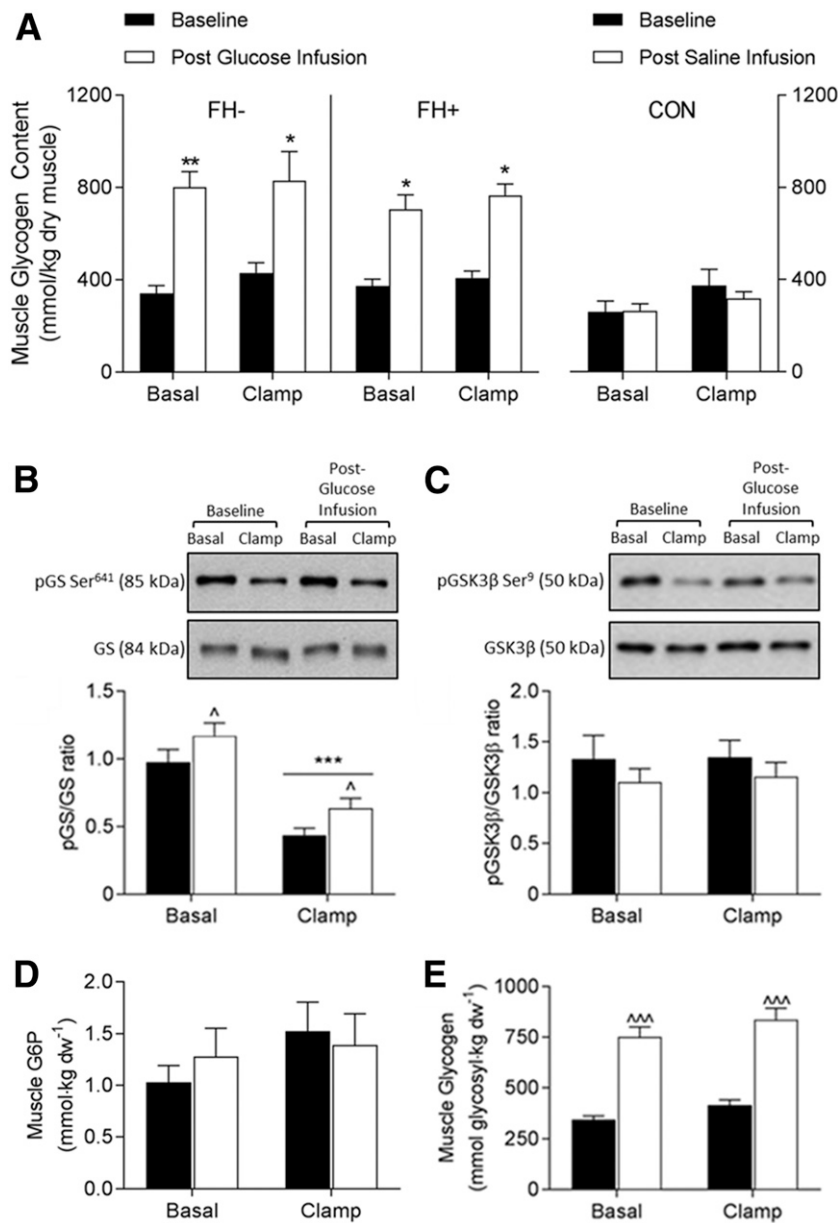
Figure 4—Glycogen synthesis signaling. *A*: Skeletal muscle glycogen content at baseline and during 3 days of either glucose infusion in NGT individuals without (FH⁻, dark bars, *n* = 10) and with (FH⁺, white bars, *n* = 10) FH of diabetes, or saline infusion in the NGT control group (right panel, *n* = 5). Representative Western blot images of the total and phosphorylated protein expression (top panel) and densitometry quantitation of the phosphorylated-to-total ratio of GS (*B*) and GSK3β (*C*). G6P (*D*) and glycogen (*E*) concentrations in skeletal muscle of all subjects receiving glucose infusion. Data are expressed as the mean ± SE and were analyzed using two-way repeated-model (clamp × infusion) ANOVA. *$P < 0.05$, **$P < 0.01$, and ***$P < 0.001$, for clamp vs. basal; ^$P < 0.05$ and ^^^$P < 0.001$, postglucose infusion vs. baseline. CON, control.

hyperglycemia also exerts a glucotoxic effect on hepatic and/or renal glucose production (34). Because the insulin infusion rate used during the insulin clamp in the current study produced a high steady-state plasma insulin concentration, EGP was near completely suppressed to the same level as that observed during the baseline insulin clamp in both groups. Although it should be acknowledged that hyperglycemia might also have influenced hepatic glucose extraction, given the relatively minor contribution of splanchnic glucose uptake to total insulin-stimulated

glucose disposal (5), it is unlikely that this was a major factor in the decrement in whole-body glucose uptake.

Since elevation of plasma glucose concentration was not performed in combination with a pancreatic/somatostatin clamp, the plasma insulin concentration also rose during the 3-day glucose infusion. We previously demonstrated that chronic elevation in plasma insulin concentration affects both oxidative and nonoxidative pathways of glucose disposal in lean healthy individuals (16). Thus, hyperinsulinemia during the 3-day glucose infusion also could
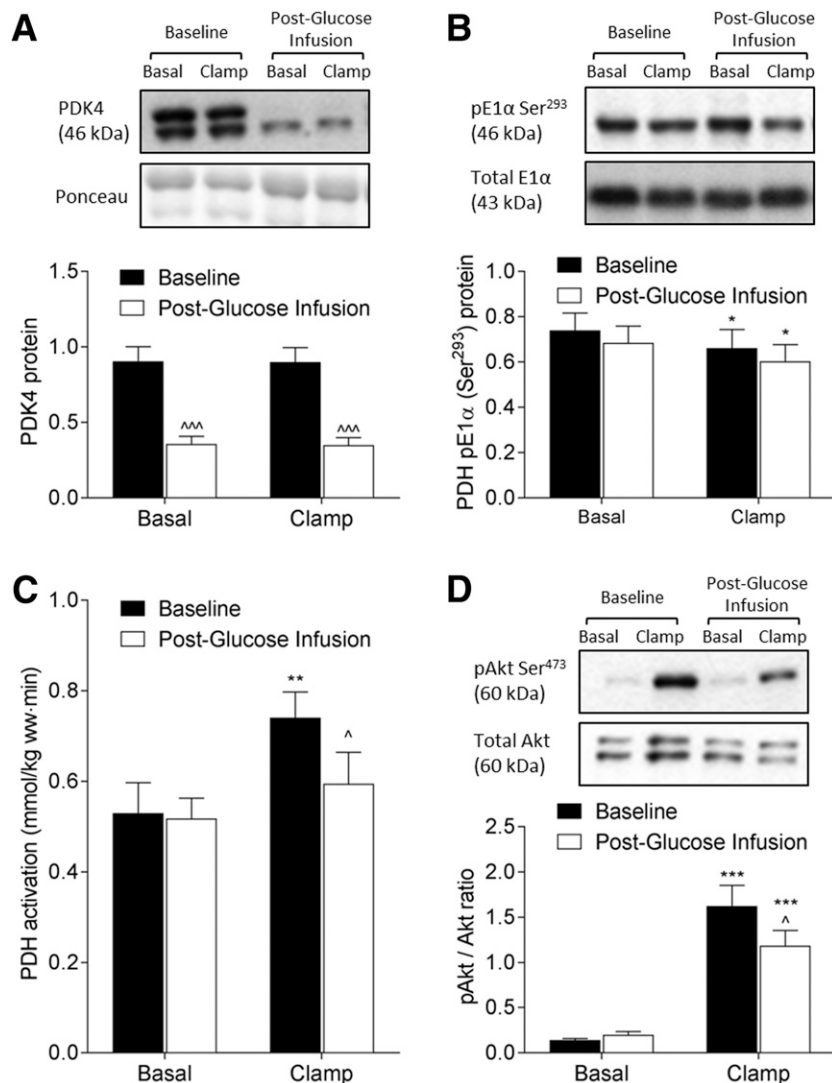
Figure 5—PDH regulation and insulin signaling. Representative Western blot images and densitometry quantitation of PDK4 protein expression (*A*), PDH E1α subunit phosphorylation (*B*), and Akt phosphorylation (*D*) and PDH activation status (*C*) at baseline (black bars) and after 3 days of glucose (white bars) infusion in NGT subjects. Data represent mean ± SE and were analyzed using two-way mixed-model (group × clamp; group × infusion) ANOVA. *$P < 0.05$, **$P < 0.01$, and ***$P < 0.001$ for clamp vs. basal; ^$P < 0.05$ and ^^^$P < 0.001$, postglucose infusion vs. baseline.

have contributed to the observed effects on oxidative and nonoxidative disposal in the current study. Nonetheless, the combined hyperglycemic (+45 mg/dL) hyperinsulinemic conditions in the current study more closely reflect the physiologic conditions observed in poorly controlled obese individuals with T2D.

The present results also shed light on the mechanisms via which chronic exposure to hyperglycemia causes skeletal muscle insulin resistance. In individuals with T2D, the principle manifestation of skeletal muscle insulin resistance is impaired insulin-mediated nonoxidative glucose disposal, which after 3 days of sustained hyperglycemia (and hyperinsulinemia) in the current study was reduced by ~50%. Nonoxidative glucose disposal primarily represents skeletal muscle glycogen synthesis (32), a process controlled by the activity of GS. Increased muscle glycogen

concentration has been shown to increase GS phosphorylation and directly inhibit GS activity (35–37), whereas the regulation of GS activity by GSK3β occurs independently from muscle glycogen content (37). Thus, both allosteric (increased glycogen) and posttranslational (phosphorylation, possibly by GSK3β) regulation of GS likely contributed to the inhibition of nonoxidative glucose disposal after 3 days of hyperglycemia. Impaired GS activity per se might normally be associated with an increase in intracellular G6P concentrations and subsequent alleviation of GS inhibition by allosterism. In the current study, G6P accumulation was likely prevented by a shunting of G6P toward glycolysis and glucose oxidation (36).

Maintenance of the intracellular G6P pool after hyperglycemia suggests that sarcolemmal glucose transport may not have been a primary defect responsible for the
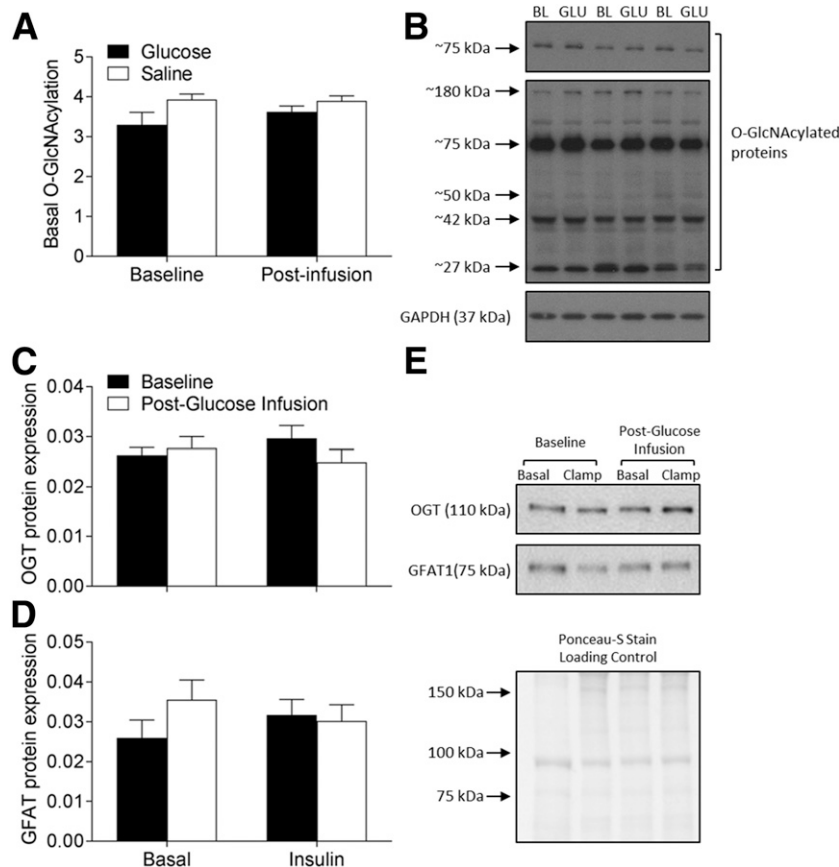
Figure 6—Basal O-GlcNAcylated protein quantification before and after 3 days of saline (white bars) or glucose (black bars) infusion (*A*) and representative blot for three subjects receiving glucose infusion (*B*). Basal and insulin-stimulated OGT (*C*) and GFAT1 (*D*) quantification before (black bars) and after (white bars) 3 days of glucose infusion and representative blots (*E*). Data represent mean ± SE and were analyzed using two-way mixed-model (group × clamp; group × infusion) ANOVA. BL, baseline; GLU, glucose.

reduction in insulin-stimulated glucose disposal. This is in contrast to what is believed to represent the rate-limiting impairment in skeletal muscle of patients with T2D and offspring (38,39). However, it is possible that changes in G6P were masked by measurement errors introduced during the tissue biopsy procedure. Moreover, insulin-stimulated Akt phosphorylation (activation) was reduced by 27% after hyperglycemia. Given that GLUT4 translocation is a primary downstream target of Akt, we cannot conclusively rule out impairment of sarcolemmal glucose transport in the development of glucotoxicity and insulin resistance with this model. Interestingly, another notable substrate for Akt in skeletal muscle is GSK3β, providing an additional mechanism through which lower Akt activity could contribute to the reduction in nonoxidative glucose disposal after hyperglycemia.

Few data exist on the regulatory role of the PDH complex in response to sustained hyperglycemia in humans. In the current study, the changes in circulating concentrations of insulin (increased) and FFA (decreased) that accompanied hyperglycemia likely contributed to the downregulation of PDK4 protein expression (40). This would be expected to favor transformation of PDH to its active form to facilitate the increase in glucose oxidation. However, neither the phosphorylation nor basal activation status of PDH were altered by glucose infusion. This discrepancy likely reflects the complex allosteric regulation of flux through the active fraction of PDH. Indeed, the marked increase in muscle glycogen concentration and inhibition of GS activity after glucose infusion would be expected to favor an increased rate of pyruvate formation and consequently augment PDH flux independently of activation status (41). Consistent with previous findings in rats (36), these results demonstrate how a defect in nonoxidative glucose disposal through perturbations in GS activity can promote the subsequent shunting of glucose through glycolysis toward oxidation. Although markedly increased, the enhanced rate of glucose oxidation was still insufficient to offset the decrement in muscle glycogen synthesis, and consequently insulin-stimulated whole-body glucose disposal was reduced. Interestingly, the ability of insulin to activate PDH was lost after glucose infusion, which was consistent with the failure of insulin to stimulate any further increase in glucose oxidation and is further indicative of distal impairments in skeletal muscle insulin action.

Another pathway that may be sensitive to the shunting of glucose from nonoxidative disposal toward glycolysis is the hexosamine synthesis pathway, which has been linked with the development of glucotoxicity and insulin resistance (20–22). However, we found no evidence for an increase in glucose metabolism to hexosamines, as reflected by stable levels of protein O-GlcNAcylation, GFAT1, and OGT in skeletal muscle. It is possible that a longer duration of hyperglycemia is needed to observe upregulation of these pathways, which have previously been shown to be increased in individuals with T2D (21). Another alternative route of glucose metabolism is through the lipid synthesis pathway, offering a mechanistic link between glucotoxicity and lipotoxicity. Indeed, RER values >1.0 were observed in many volunteers after glucose infusion, indicative of whole-body net lipid synthesis. However, given the sustained suppression of circulating FFA during the glucose infusion, and consistent with the lack of effect on LCAC concentrations, the contribution of lipogenesis (presumably hepatic) and change in plasma lipid levels to the development of skeletal muscle insulin resistance is likely to be inconsequential.

In summary, the current study demonstrates that sustained physiologic hyperglycemia for 3 days produces marked insulin resistance in the nonoxidative (glycogen synthesis) pathway of glucose disposal while augmenting the glucose oxidative pathway. At the molecular level, perturbations in both GS and PDH activation play an important role in the glucotoxic effect of hyperglycemia to produce insulin resistance.

References

1. Defronzo RA. Banting Lecture. From the triumvirate to the ominous octet: a new paradigm for the treatment of type 2 diabetes mellitus. Diabetes 2009;58: 773–795

2. DeFronzo RA, Ferrannini E, Groop L, et al. Type 2 diabetes mellitus. Nat Rev Dis Primers 2015;1:15019

3. Gulli G, Ferrannini E, Stern M, Haffner S, DeFronzo RA. The metabolic profile of NIDDM is fully established in glucose-tolerant offspring of two Mexican-American NIDDM parents. Diabetes 1992;41:1575–1586

4. Martin BC, Warram JH, Krolewski AS, Bergman RN, Soeldner JS, Kahn CR. Role of glucose and insulin resistance in development of type 2 diabetes mellitus: results of a 25-year follow-up study. Lancet 1992;340:925–929

5. DeFronzo RA, Gunnarsson R, Björkman O, Olsson M, Wahren J. Effects of insulin on peripheral and splanchnic glucose metabolism in noninsulin-dependent (type II) diabetes mellitus. J Clin Invest 1985;76:149–155

6. Bajaj M, Baig R, Suraamornkul S, et al. Effects of pioglitazone on intramyocellular fat metabolism in patients with type 2 diabetes mellitus. J Clin Endocrinol Metab 2010;95:1916–1923

7. Clarke GD, Solis-Herrera C, Molina-Wilkins M, et al. Pioglitazone improves left ventricular diastolic function in subjects with diabetes. Diabetes Care 2017; 40:1530–1536

8. Gastaldelli A, Gaggini M, DeFronzo RA. Role of adipose tissue insulin resistance in the natural history of type 2 diabetes: results from the San Antonio Metabolism Study. Diabetes 2017;66:815–822

9. DeFronzo RA, Ferrannini E, Simonson DC. Fasting hyperglycemia in non-insulin-dependent diabetes mellitus: contributions of excessive hepatic glucose production and impaired tissue glucose uptake. Metabolism 1989;38:387–395

10. Mäkinen J, Hannukainen JC, Karmi A, et al. Obesity-associated intestinal insulin resistance is ameliorated after bariatric surgery. Diabetologia 2015;58:1055–1062

11. Groop LC, Bonadonna RC, DelPrato S, et al. Glucose and free fatty acid metabolism in non-insulin-dependent diabetes mellitus. Evidence for multiple sites of insulin resistance. J Clin Invest 1989;84:205–213

12. Felber JP, Ferrannini E, Golay A, et al. Role of lipid oxidation in pathogenesis of insulin resistance of obesity and type II diabetes. Diabetes 1987;36:1341–1350

13. Rossetti L, Smith D, Shulman GI, Papachristou D, DeFronzo RA. Correction of hyperglycemia with phlorizin normalizes tissue sensitivity to insulin in diabetic rats. J Clin Invest 1987;79:1510–1515

14. Kahn BB, Shulman GI, DeFronzo RA, Cushman SW, Rossetti L. Normalization of blood glucose in diabetic rats with phlorizin treatment reverses insulin-resistant glucose transport in adipose cells without restoring glucose transporter gene expression. J Clin Invest 1991;87:561–570

15. Yki-Järvinen H, Helve E, Koivisto VA. Hyperglycemia decreases glucose uptake in type I diabetes. Diabetes 1987;36:892–896

16. Del Prato S, Leonetti F, Simonson DC, Sheehan P, Matsuda M, DeFronzo RA. Effect of sustained physiologic hyperinsulinaemia and hyperglycaemia on insulin secretion and insulin sensitivity in man. Diabetologia 1994;37:1025–1035

17. Rossetti L, Giaccari A, DeFronzo RA. Glucose toxicity. Diabetes Care 1990;13: 610–630

18. Garvey WT, Olefsky JM, Griffin J, Hamman RF, Kolterman OG. The effect of insulin treatment on insulin secretion and insulin action in type II diabetes mellitus. Diabetes 1985;34:222–234

19. Merovci A, Solis-Herrera C, Daniele G, et al. Dapagliflozin improves muscle insulin sensitivity but enhances endogenous glucose production. J Clin Invest 2014;124:509–514

20. Yki-Järvinen H, Vogt C, Iozzo P, et al. UDP-N-acetylglucosamine transferase and glutamine: fructose 6-phosphate amidotransferase activities in insulin-sensitive tissues. Diabetologia 1997;40:76–81

21. Yki-Järvinen H, Daniels MC, Virkamäki A, Mäkimattila S, DeFronzo RA, McClain D. Increased glutamine:fructose-6-phosphate amidotransferase activity in skeletal muscle of patients with NIDDM. Diabetes 1996;45:302–307

22. Yki-Järvinen H, Virkamäki A, Daniels MC, McClain D, Gottschalk WK. Insulin and glucosamine infusions increase O-linked N-acetyl-glucosamine in skeletal muscle proteins in vivo. Metabolism 1998;47:449–455

23. Parker G, Taylor R, Jones D, McClain D. Hyperglycemia and inhibition of glycogen synthase in streptozotocin-treated mice: role of O-linked N-acetylglucosamine. J Biol Chem 2004;279:20636–20642

24. Burnham-Marusich AR, Berninsone PM. Multiple proteins with essential mitochondrial functions have glycosylated isoforms. Mitochondrion 2012;12:423–427

25. Kashyap S, Belfort R, Gastaldelli A, et al. A sustained increase in plasma free fatty acids impairs insulin secretion in nondiabetic subjects genetically predisposed to develop type 2 diabetes. Diabetes 2003;52:2461–2474

26. DeFronzo RA, Tobin JD, Andres R. Glucose clamp technique: a method for quantifying insulin secretion and resistance. Am J Physiol 1979;237:E214–E223

27.   Constantin-Teodosiu D, Cederblad G, Hultman E. A sensitive radioisotopic assay of pyruvate dehydrogenase complex in human muscle tissue. Anal Biochem 1991;198:347–351

28.   Harris RC, Hultman E, Nordesjö L-O. Glycogen, glycolytic intermediates and high-energy phosphates determined in biopsy samples of musculus quadriceps femoris of man at rest. Methods and variance of values. Scand J Clin Lab Invest 1974;33:109–120

29.   Cederblad G, Carlin JI, Constantin-Teodosiu D, Harper P, Hultman E. Radioisotopic assays of CoASH and carnitine and their acetylated forms in human skeletal muscle. Anal Biochem 1990;185:274–278

30.   Ferrannini E, Smith JD, Cobelli C, Toffolo G, Pilo A, DeFronzo RA. Effect of insulin on the distribution and disposition of glucose in man. J Clin Invest 1985;76:357–364

31.   Simonson DC, DeFronzo RA. Indirect calorimetry: methodological and interpretative problems. Am J Physiol 1990;258:E399–E412

32.   Shulman GI, Rothman DL, Jue T, Stein P, DeFronzo RA, Shulman RG. Quantitation of muscle glycogen synthesis in normal subjects and subjects with non-insulin-dependent diabetes by ^{13}C nuclear magnetic resonance spectroscopy. N Engl J Med 1990;322:223–228

33.   McClain DA, Crook ED. Hexosamines and insulin resistance. Diabetes 1996; 45:1003–1009

34.   DeFronzo RA, Norton L, Abdul-Ghani M. Renal, metabolic and cardiovascular considerations of SGLT2 inhibition. Nat Rev Nephrol 2017;13:11–26

35.   Danforth WH. Glycogen synthetase activity in skeletal muscle. Interconversion of two forms and control of glycogen synthesis. J Biol Chem 1965;240:588–593

36.   Jensen J, Jebens E, Brennesvik EO, et al. Muscle glycogen inharmoniously regulates glycogen synthase activity, glucose uptake, and proximal insulin signaling. Am J Physiol Endocrinol Metab 2006;290:E154–E162

37.   Lai Y-C, Stuenaes JT, Kuo CH, Jensen J. Glycogen content and contraction regulate glycogen synthase phosphorylation and affinity for UDP-glucose in rat skeletal muscles. Am J Physiol Endocrinol Metab 2007;293:E1622–E1629

38.   Rothman DL, Magnusson I, Cline G, et al. Decreased muscle glucose transport/phosphorylation is an early defect in the pathogenesis of non-insulin-dependent diabetes mellitus. Proc Natl Acad Sci U S A 1995;92:983–987

39.   Rothman DL, Shulman RG, Shulman GI. 31P nuclear magnetic resonance measurements of muscle glucose-6-phosphate. Evidence for reduced insulin-dependent muscle glucose transport or phosphorylation activity in non-insulin-dependent diabetes mellitus. J Clin Invest 1992;89:1069–1075

40.   Chokkalingam K, Jewell K, Norton L, et al. High-fat/low-carbohydrate diet reduces insulin-stimulated carbohydrate oxidation but stimulates nonoxidative glucose disposal in humans: an important role for skeletal muscle pyruvate dehydrogenase kinase 4. J Clin Endocrinol Metab 2007;92:284–292

41.   Constantin-Teodosiu D, Peirce NS, Fox J, Greenhaff PL. Muscle pyruvate availability can limit the flux, but not activation, of the pyruvate dehydrogenase complex during submaximal exercise in humans. J Physiol 2004;561:647–655